RSC Advances

RSCPublishing

PAPER

View Article Online
View Journal | View Issue

Cite this: *RSC Advances*, 2013, **3**, 5583

Novel bi-functional Ni–Mg–Al–CaO catalyst for catalytic gasification of biomass for hydrogen production with *in situ* CO_2 adsorption

Mohamad A. Nahil,[a] Xianhua Wang,[b] Chunfei Wu,[a] Haiping Yang,[b] Hanping Chen*[b] and Paul T. Williams*[a]

Received 16th November 2012,
Accepted 6th February 2013

DOI: 10.1039/c3ra40576a

www.rsc.org/advances

Catalytic gasification of biomass in the presence of CaO is a promising route for CO_2 capture and thereby high yield hydrogen production. However, the instability of the CaO sorbent for CO_2 adsorption is a challenge for the process. A novel bi-functional Ni–Mg–Al–CaO catalyst has been prepared with different contents of CaO by integration of the catalytic and CO_2 adsorbing materials to maximise hydrogen production. The prepared catalysts were tested for hydrogen production *via* the pyrolysis-gasification of wood biomass using a two-stage fixed-bed reaction system. The carbonation/calcination results using thermogravimetric analysis (TGA), in an atmosphere of N_2 or CO_2, showed that the reactivity of CaO with CO_2 decreased even after several cycles of carbonation/calcination, while the Ni–Mg–Al–CaO catalyst showed a comparatively stable CO_2 adsorption even after 20 cycles. Adding CaO to the Ni–Mg–Al catalyst leads to an increase in hydrogen production and selectivity due to the enhancement of the water–gas shift reaction by *in situ* CO_2 adsorption. An optimal content of CaO was suggested to be 20 wt% (weight ratio of CaO/Ni–Mg–Al) which gave the highest hydrogen production (20.2 mmol g^{-1} biomass) in the presence of the Ni–Mg–Al–CaO catalyst. Temperature-programmed oxidation (TPO) showed that carbon deposition was significantly decreased with the addition of CaO in the Ni–Mg–Al catalyst, and with the increase of CaO content, coke deposition on the reacted catalyst was further decreased.

1. Introduction

There is increasing worldwide research and development into the sustainable and efficient production of energy from renewable sources.[1] Biomass is one of the important primary and renewable energy sources and is classified as the third energy source in terms of usage after coal and oil.[2,3] In addition, hydrogen is a promising energy source that can partially replace fossil energy and is predicted to play an important role in future energy systems. Currently, hydrogen is industrially produced by the conversion of fossil fuels, but has a low conversion efficiency and releases greenhouse gases during the process.[4] Production of hydrogen from renewable resources, such as biomass, would provide a sustainable route for hydrogen production using a source which is carbon neutral.

Hydrogen production has been extensively studied *via* the pyrolysis-gasification of biomass.[5–7] Many catalysts have also been investigated for biomass gasification to improve the efficiency of the process and increase hydrogen production.[7–9] Ni-based catalysts have been reported to be effective for hydrogen production from biomass gasification with significantly lower costs compared to noble metal catalysts, such as Ru and Rh. In addition, the steam gasification of biomass, in the presence of a calcium oxide (CaO) sorbent for CO_2 capture, is an innovative pathway to improve H_2 yield compared to conventional gasification.[10–12]

Steam gasification of biomass pyrolysis hydrocarbons consists of two main reactions:

Hydrocarbons reforming reaction:

$$C_nH_mO_z + (n - z)\,H_2O \rightarrow nCO + (n - z + m/2)\,H_2 \quad (1)$$

Water–gas shift reaction:

$$CO + H_2O \leftrightarrow CO_2 + H_2 \quad (2)$$

Calcium oxide could be used to adsorb the produced CO_2 and release heat *via* the following reaction:

$$CaO + CO_2 \rightarrow CaCO_3 \quad (3)$$

The concept of using sorbents combines hydrocarbon reforming, water–gas shift and CO_2 adsorption reactions into

---

[a] *Energy Research Institute, The University of Leeds, Leeds, LS2 9JT, UK. E-mail: p.t.williams@leeds.ac.uk; Tel: +44 1133432504*

[b] *State Key Laboratory of Coal Combustion, Huazhong University of Science and Technology, Wuhan, 430074, China. E-mail: hp.chen@163.com; Tel: +86 27 87559358*

a single step, as reported in previous studies.[11,13] During the gasification, in the presence of a CO_2 sorbent, the gasification of hydrocarbons (eqn (1)) is enhanced at high temperature, while the water–gas shift reaction (eqn (2)) and CO_2 adsorption reaction (eqn (3)) are inhibited due to the exothermic properties of the two reactions. The presence of a catalyst, along with a CO_2 sorbent, could reduce the gasification temperature for hydrogen production, thus favouring the reactions in eqn (2) and (3). Therefore, the combination of a Ni-based catalyst and CO_2 sorbent provides a promising way to increase the efficiency of biomass gasification in terms of hydrogen production. However, the deactivation of the CO_2 sorbent, normally CaO, is a challenge for the application of CO_2 capture during the biomass gasification.[14,15]

Here, we have prepared a novel catalyst by incorporating a CO_2 sorbent (CaO) into a Ni-based catalyst (Ni–Mg–Al) to improve the stability of CaO in relation to CO_2 adsorption. The bi-functional catalyst (Ni–Mg–Al–CaO) was evaluated for hydrogen production from the pyrolysis-gasification of biomass using a fixed-bed two-stage reaction system.

2. Materials and methods

2.1 Materials

Wood biomass, with a particle size of less than 200 μm, was used in the experiments as a representative biomass sample. The elemental analysis (C, H, N, S) of the wood was carried out using a Carlo Erba Flash EA 1112 elemental analyser, while the oxygen content was determined by the difference.

A Shimadzu TGA-50H analyser was used to perform the proximate analysis of the wood sample. Heating of the sample in a nitrogen atmosphere to 110 °C at a heating rate of 25 °C min^{-1} and a hold time of 10 min corresponded to the determination of moisture in the sample; heating to 925 °C produced a weight loss corresponding to the content of the volatile matter; the fixed carbon content was determined by the introduction of air which burns off the fixed carbon in the sample, leaving the ash residue. The compositions of the samples are shown in Table 1.

A precursor of the Ni–Mg–Al catalyst was first prepared using the rising pH technique according to the method reported by Garcia *et al.*[16] The precipitant, 1 M $NH_4(OH)$, was added to 200 ml of an aqueous solution containing $Ni(NO_3)\cdot 6H_2O$, $Mg(NO_3)_2\cdot 6H_2O$ and $Al(NO_3)_3\cdot 9H_2O$. The precipitation was carried out at 40 °C with moderate stirring until a final pH of 8.3 was obtained. The precipitates were filtered with water (40 °C), then CaO was added (Sigma Aldrich) and mixed well. The precursor of Ni–Mg–Al–CaO was dried at 105 °C overnight, and then calcined at 750 °C for 3 h. The Ni–Mg–Al molar ratio was 1 : 1 : 1. Certain amounts of CaO (0.5, 1, 2, and 3 g) were added to the Ni–Mg–Al (4 g) catalyst which represented 12.5, 25, 50 and 75 wt% of the weight of the Ni–Mg–Al catalyst after calcination. The Ni–Mg–Al catalyst mixed with quartz (Ni–Mg–Al–1Quartz) was also tested to compare its activity with the Ni–Mg–Al–CaO catalyst.

The Ni–Mg–Al catalyst, without the CaO, was also prepared under the same conditions. The catalysts used in this research were crushed and sieved to granules with a size ranging between 65 and 212 μm. The nomenclature used in this paper for the prepared catalyst is as follows: Ni–Mg–Al denotes the catalyst, followed by the amount of added CaO. For example, Ni–Mg–Al–0.5CaO equates to Ni–Mg–Al catalyst mixed with 0.5 g of CaO.

Table 1 Elemental and proximate analysis of the wood biomass

Elemental analysis (wt%)			
C	**H**	**N**	**O**[a]
47.1	5.9	0.1	46.9
Proximate analysis (wt%)			
Moisture	**Volatiles**	**Fixed carbon**	**Ash**
6.2	74.6	18.1	1.1

[a] Calculated by the difference.

2.2 Catalyst characterisation

The carbonation/calcination experiments of the produced catalyst (Ni–Mg–Al–CaO) and CaO were carried out using a WRT-2C, Beijing Optical Instrument Factory thermogravimetric analyser (TGA) to investigate the stability of the sorbent/catalyst for CO_2 capture. Around 10 mg of sorbent was first heated in an atmosphere of pure CO_2 at 30 °C min^{-1} to a final temperature of 800 °C. Then the flow gas was changed to N_2, at a rate of 100 ml min^{-1} and temperature of 800 °C, where the adsorption of CO_2 was completed. More than 20 carbonation/calcination cycles were investigated.

A Quanta 200, FEI scanning electron microscope was used to analyse the surface of the CO_2 sorbent/catalysts after the carbonation/calcination experiments. The surface characteristics of the CO_2 sorbent/catalysts used during the pyrolysis-gasification experiments were determined using a high resolution LEO 1530 FEG scanning electron microscope coupled to an energy dispersive X-ray spectrometer (EDXS) system. In addition, EDXS was also used for a semi-quantitative elemental analysis of the fresh CO_2 sorbent/catalysts.

The carbon deposited on the used catalysts was examined by temperature-programmed oxidation (TPO) carried out using a Stanton-Redcroft thermogravimetric analyser (TGA) interfaced with a Nicolet Magna IR-560 Fourier transform infra-red spectrometer (FTIR). The catalyst sample of approximately 200 mg was placed in the TGA and heated at 15 °C min^{-1} in air, and the weight loss was recorded up to a sample temperature of 800 °C with a final hold time of 10 min. The sample weight loss, together with time, temperature, and volatile species detected by FTIR, were continuously monitored.

2.3 Experimental pyrolysis-catalytic steam gasification system

Testing of the prepared Ni–Mg–Al–CaO catalysts with the purpose of maximising hydrogen production and adsorption of CO_2 from the pyrolysis-gasification of wood was carried out in a two-stage reaction system (Fig. 1). The two-stage fixed-bed reaction system consisted of a pre-heated stage and a gasification stage. The wood sample was pyrolysed in the first stage, and the pyrolysis products were passed directly into a second stage where the steam catalytic gasification of the

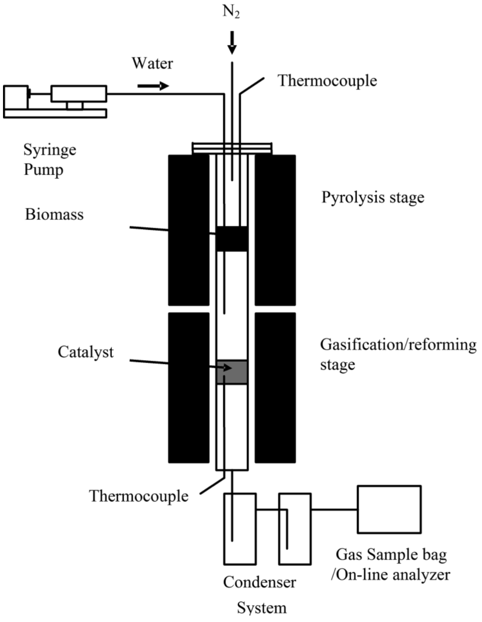

Fig. 1 Schematic diagram of the two stage pyrolysis-catalytic gasification experimental system.

pyrolysis gases was carried out. The wood sample mass used in each experiment was approximately 2.0 g and the catalyst mass was 1.0 g. The experimental procedure consisted of initial heating of the catalyst in the second stage gasification reactor to 800 °C; once the temperature of the second stage gasification reactor had stabilised, the wood sample was pyrolysed at a heating rate of 25 °C min^{-1} to the final pyrolysis temperature of 600 °C in the first stage reactor and held at this temperature for 40 min. The evolved pyrolysis volatiles were passed directly to the second stage where water was also introduced and thereby the pyrolysis volatiles reacted with the catalyst in the presence of steam to produce the steam catalytic gasification conditions. Two condensers were used to trap the condensable products, consisting of an air cooled condenser, followed by a solid CO_2 cooled condenser.

The non-condensed gases were collected with a 25 L Tedlar TM gas sample bag. The gases collected in the sample bag were analysed off-line by packed column gas chromatography (GC). Hydrocarbon gases (C_1–C_4) were analysed using a Varian CP-3380 gas chromatograph with a Flame Ionisation Detector (FID). The column was stainless steel, 2 m long, 2 mm diameter packed with 80–100 mesh size Haysep. The carrier gas used was nitrogen.

Carbon dioxide, hydrogen, nitrogen, carbon monoxide and oxygen were analysed with a separate Varian CP-3380 gas chromatograph fitted with a thermal conductivity detector (TCD), with two packed columns. A 2 m long and 2 mm diameter column packed with 60–80 mesh molecular sieves was used to analyse the hydrogen, nitrogen, carbon monoxide and oxygen, while the carbon dioxide was analysed on a 2 m long and 2 mm diameter column with Haysep 60–80 mesh molecular sieves. The carrier gas was argon.

An on-line gas analyser (ABB Systems, UK) was also used to record on-line hydrogen, methane, carbon dioxide and carbon monoxide products respectively at 5 s intervals for the selected catalyst/sorbent samples. H_2 was measured by a thermal conductivity detector and CO, CO_2 and CH_4 *via* non-dispersive infra-red absorption-based instruments.

H_2 selectivity (HS) was calculated according to eqn (4):

$$\text{HS} = \frac{\text{moles } H_2}{\text{moles } H_2 + \text{moles CO} + \text{moles shydrocarbons}(C_1 \text{ to } C_4)} \times 100 \quad (4)$$

3. Results and discussion

3.1 Carbonation/calcination of the sorbents with TGA

The performance of the selected CO_2 sorbents, including CaO and the prepared Ni–Mg–Al catalyst with different contents of CaO, were tested for their carbonation conversion using TGA. Cyclical studies were carried out to evaluate any loss in reactivity of these sorbents after multiple cycles. The results

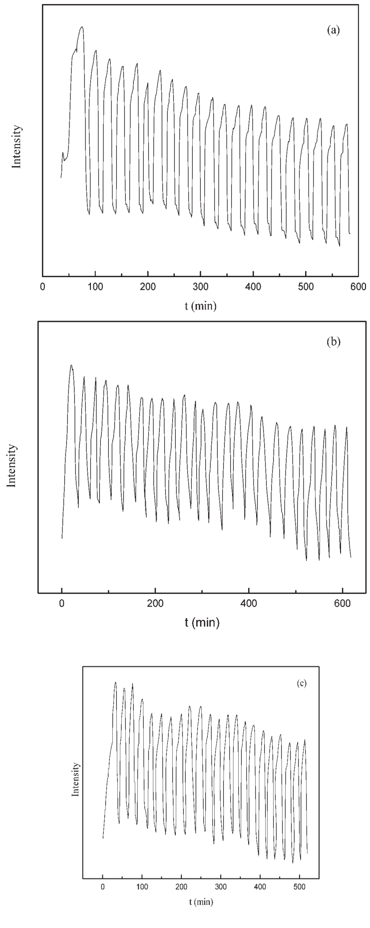

Fig. 2 TGA curves recorded during the carbonation/calcination reaction cycles of different CO_2 sorbents (a) CaO, (b) Ni–Mg–Al–2CaO and (c) Ni–Mg–Al–3CaO.

for at least 20 carbonation/calcination cycles are shown in Fig. 2.

It can be seen that the reactivity of CaO exhibited a gradual decrease after several carbonation/calcination cycles in atmospheres of N_2 or CO_2. The reduction in the efficiency of CO_2 adsorption for the CaO sample was around 40%. The efficiency loss of CO_2 adsorption was calculated as follows:

$$CO_2 \text{ adsorption efficiency loss} = (P_L - P_0)/P_0 \times 100, \quad (5)$$

where 'P' (CO_2 adsorption percentage) equals the weight of adsorbed CO_2 divided by the weight of the adsorbent. P_L and P_0 are assigned to the last and first carbonation/calcination cycle of TGA analysis, respectively.

The decrease in the efficiency of CO_2 adsorption for CaO has also been reported by other researchers.[11,17,18] According to Alvarez and Abanades,[19] the decrease in the reactivity of CaO was attributed to the sintering of CaO. In addition, Lu *et al.*[20] reported that longer durations at higher temperatures damages the structural nature of CaO. Fig. 3 shows a scanning electron mircoscopy (SEM) micrograph of the fresh CaO, and CaO after carbonation/calcination. The SEM micrographs suggest that the pore size of the CaO is increased after the carbonation/calcination cycles, which may indicate that the microporosity decreased with a corresponding increase in the mesoporosity and macroporosity of the CaO. The presence of larger pores results in the reduction of the reactivity of CaO, since it decreases the surface area.

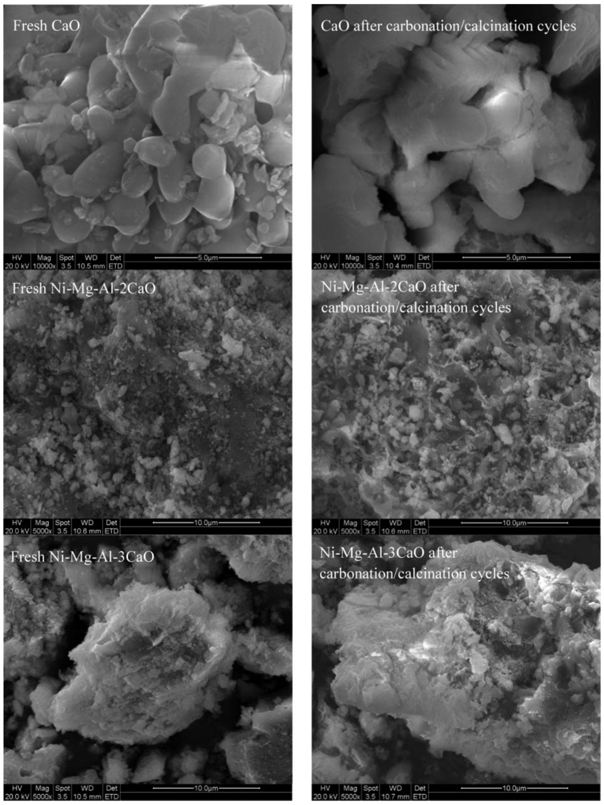

Fig. 3 SEM results of the fresh and tested (after multiple carbonation/calcination cycles with TGA) CO_2 capture sorbents.

In contrast to the CaO carbonation/calcination results, the prepared catalyst/sorbent, Ni–Mg–Al–2CaO and Ni–Mg–Al–3CaO, showed similar surface morphologies compared with the pure CaO sorbent after the calcination/carbonation cycles, suggesting a more stable catalyst. Fig. 3 also shows that the sintering that took place for the pure CaO sorbent did not occur for the Ni–Mg–Al–CaO catalyst, according to the catalyst/sorbent morphology. Therefore, the incorporation of CaO into the Ni–Mg–Al catalyst system has been shown to improve the stability of the catalyst/sorbent for CO_2 capture, compared with the pure CaO sorbent.

3.2 The effect of CaO addition to the Ni–Mg–Al catalyst on the gas yield and composition

3.2.1 Gas analysis. The bi-functional Ni–Mg–Al catalyst with different amounts of CaO, 0, 0.5, 1, 2 and 3 g, which represented 0, 11.1, 20, 33.3 and 42.9 wt% of the weight of the Ni–Mg–Al–CaO catalyst, were investigated for hydrogen production and CO_2 adsorption *via* the pyrolysis catalytic gasification of wood using the laboratory scale fixed-bed reaction system. The gas yield and the gas composition produced with and without the catalysts are shown in Table 2. The gas yield was calculated as the weight of gases in relation to the weight of wood biomass.

The data shown in Table 2 indicates that there were significant changes in the gas yields and the composition of the gaseous products when the Ni–Mg–Al catalyst was used, regardless of the CaO content. For example, the gas yield and the H_2 production were increased from 40.7 to 64.2 wt% and 3.6 to 20.4 (mmol H_2 g^{-1} biomass) respectively, when the Ni–Mg–Al catalyst was added to the second stage gasification reactor.

Although the hydrogen and gas production, in terms of the weight of biomass, were slightly reduced when the catalyst was changed from Ni–Mg–Al to Ni–Mg–Al–CaO, the hydrogen production related to the CO production was increased with the increased addition of CaO in the catalyst system (Table 2). For example, the H_2/CO ratio was increased from 0.128 to 0.137 (g g^{-1}) when the Ni–Mg–Al catalyst was replaced by the Ni–Mg–Al–0.5CaO catalyst; the ratio of H_2/CO was further increased to 0.160 (g g^{-1}) when the CaO content was increased from 11.1 to 42.9 wt%. It is suggested that the water–gas shift reaction (eqn (2)) was favoured in the presence of the CaO sorbent, which adsorbed CO_2 during the reforming process and resulted in a higher conversion of CO to H_2. The presence of CaO has been known to increase H_2 production during the gasification process. [15,21,22] The lower amount of hydrogen production for the Ni–Mg–Al–CaO catalyst, compared to the Ni–Mg–Al catalyst, was due to the dilution of the catalytic metals by the addition of CaO. Semi-quantity analysis using EDXS to the catalysts (Table 2) has shown that the Ni content was reduced from 14.0 to 3.4 mol% when 42.9 wt% CaO was presented in the Ni–Mg–Al catalyst system.

In order to support the advantage of the Ni–Mg–Al–CaO catalyst, a mixture of the Ni–Mg–Al catalyst and quartz (Ni–Mg–Al–Quartz), possessing similar metal contents to Ni–Mg–Al–1CaO, was tested for biomass gasification. The results confirmed that the gas yield, hydrogen production and

Table 2 Product yields and the gas composition from the pyrolysis-gasification of wood biomass

Catalyst	Blank	Ni–Mg–Al	Ni–Mg–Al–0.5CaO	Ni–Mg–Al–1Quartz	Ni–Mg–Al–1CaO	Ni–Mg–Al–2CaO	Ni–Mg–Al–3CaO
CaO content[a] (wt.%)	—	0	11.1	—	20	33.3	42.9
Ni (mol.%)	—	14.0	11.7	10.5	9.8	6.2	3.4
Mg (mol.%)	—	12.2	11.0	9.1	7.5	5.6	3.8
Al (mol.%)	—	10.9	9.7	8.2	8.5	6.1	4.3
O (mol.%)	—	62.9	64.2	—	68.0	72.6	77.4
Ca (mol.%)	—	—	3.4	—	6.2	9.5	11.1
Conversion (wt.%)[b]	66.5	66.0	65.5	65.5	64.0	64.5	64.0
Gas yield (wt.%)	40.7	64.2	54.5	51.9	60.9	56.4	54.3
Hydrogen (mmol g^{-1} biomass)	3.6	20.4	15.3	14.9	20.2	14.4	13.7
H_2/CO (g g^{-1})	0.037	0.128	0.137	0.099	0.138	0.149	0.160
Hydrogen selectivity (%)	23.4	63.2	59.6	55.8	63.7	60.9	59.1
Gas concentrations (vol.%)							
CO	38.3	29.8	25.8	35.3	28.1	22.9	20.9
H_2	19.9	52.9	49.0	48.6	53.9	47.4	46.4
CO_2	14.7	16.0	17.6	12.6	15.2	22.0	21.4
CH_4	21.4	1.2	5.9	2.8	2.1	6.0	8.9
C_2–C_4	5.7	0.1	1.8	0.7	0.7	1.7	2.5

[a] CaO content was calculated as the weight of CaO divided by the weight of the Ni–Mg–Al–CaO catalyst (wt%). [b] Conversion is calculated as (100 wt% − residue wt%).

hydrogen selectivity were increased from 51.9 to 60.9 wt%, 14.9 to 20.2 (mmol g^{-1} biomass) and 55.8 to 63.7% respectively, when quartz was replaced by CaO.

Investigation into the influence of the CaO content showed that a maximum hydrogen production (20.2 mmol g^{-1} biomass) was obtained with the Ni–Mg–Al–1CaO catalyst (20 wt% of CaO) (Table 2). This hydrogen production value is higher compared to other reports for catalytic biomass gasification.[6,7] In addition, lower hydrogen production with the CaO containing catalyst was also obtained compared to biomass gasification with the Ni–Mg–Al catalyst. The reduction of the content of the Ni–Mg–Al catalyst in the catalyst system (diluted by CaO in the catalyst system) was ascribed to the lower production of hydrogen, when CaO was added to the Ni–Mg–Al catalyst. H_2 selectivity was increased from 59.6% to 63.7% when the CaO content was increased from 11.1 to 20 wt%; with further increases of the CaO content to 42.9 wt%, the H_2 selectivity decreased slightly as a result of the catalyst being diluted by CaO.

In this work, hydrogen production was suggested to be controlled by two main routes: the catalytic steam conversion of hydrocarbons, and the water–gas shift reactions enhanced by CO_2 adsorption (as shown in Fig. 4). For example, hydrogen production was reduced when 11.1 wt% of CaO was included in the Ni–Mg–Al–0.5CaO system compared with the Ni–Mg–Al catalyst; this is due to the reduction of catalytic conversion of hydrocarbons into hydrogen with reduced catalytic sites (reduction of Ni content is observed from Table 2 when CaO was increased). With increased CaO contents (20 wt%, Ni–Mg–Al–1CaO), the water–gas shift reaction was suggested to be more dominant for hydrogen production, which was enhanced by *in situ* CO_2 adsorption; and thus resulted in higher hydrogen production (20.2 mmol g^{-1} biomass) compared with the Ni–Mg–Al–0.5CaO catalyst. However, with further increases of the CaO content, to 33.3 and 42.9 wt%, the reduction of the number of catalytic Ni sites (Table 2), due to dilution of CaO in the catalyst/sorbent, resulted in lower hydrogen production (Table 2). This can be explained by the fact that the CaO content existing in the Ni–Mg–Al–2CaO and Ni–Mg–Al–3CaO catalysts were unable to compensate for the reduction in hydrogen production resulting from the decrease in Ni content.

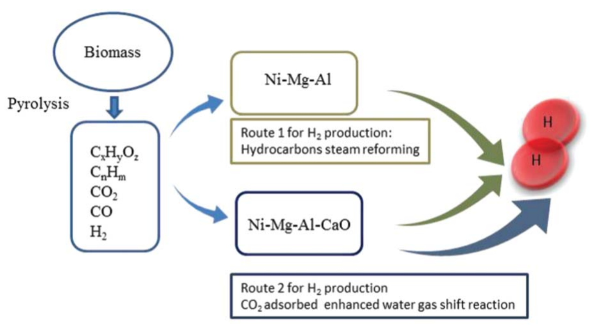

Fig. 4 Schematic diagram for hydrogen production during biomass gasification.

In order to understand the changes of gas concentration due to the influence of catalytic reforming and CO_2 adsorption during the process of biomass gasification, the online gas analyser was used for obtaining the concentrations of CH_4, H_2, CO and CO_2 for selected experiments. Gases were analysed on a continuous basis throughout the biomass pyrolysis process as the biomass was heated up to the final pyrolysis temperature. Fig. 5 shows the evolution rate of the gases *versus* time over different catalyst/sorbents (Ni–Mg–Al–0.5CaO and Ni–Mg–Al–2CaO) when the sample pyrolysis and gasification temperatures were kept at 600 and 800 °C, respectively.

For both catalyst/sorbent samples, the gases were evolved at a time of 13 min, which corresponds to a pyrolysis temperature of 300 °C. The main evolution of all gases occurred in a single stage with a maximum outflow at 15 min, which corresponds to a temperature of 350 °C. With increasing CaO content, a second peak for CO_2 with a maximum outflow at 65 min was observed as shown in Fig. 5(b). This was

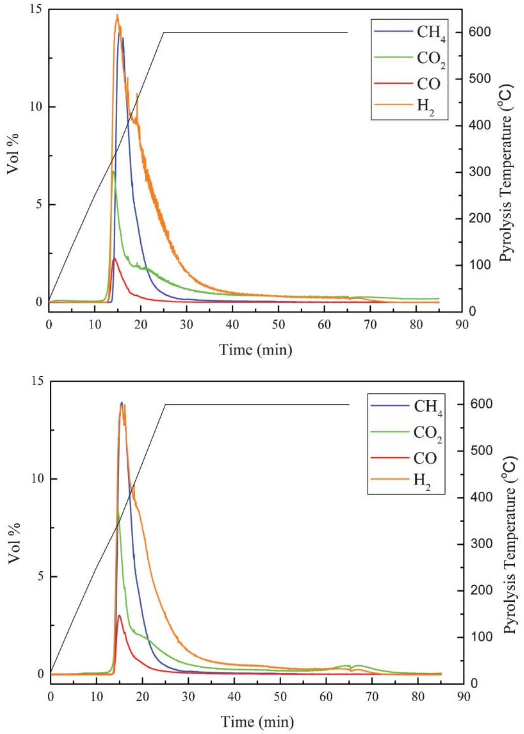

Fig. 5 Evolution rates of gases from pyrolysis-gasification of wood against time over (a) Ni–Mg–Al–0.5CaO and (b) Ni–Mg–Al–2CaO.

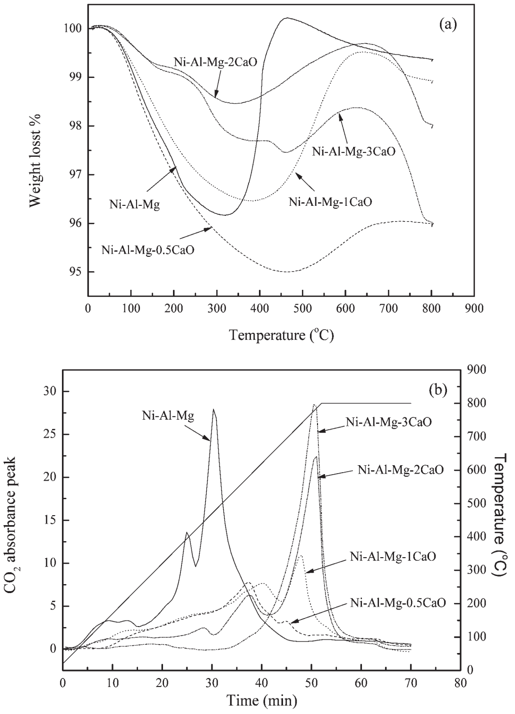

Fig. 6 TGA-TPO (a) and TGA-CO$_2$ absorbance peak (b) results of the reacted Ni–Mg–Al catalyst with different contents of CaO.

assigned to the CO$_2$ emission from reaction described in eqn (6), when the pyrolysis/gasification of biomass was carried out at 800 °C:

$$CaCO_3 \longrightarrow CaO + CO_2 \qquad (6)$$

For the gas release around 15 min, concentrations of CH$_4$ and H$_2$ were similar for the Ni–Mg–Al–0.5CaO and Ni–Mg–Al–2CaO catalysts; however, the CO and CO$_2$ concentrations were reduced at an evolution time of around 15 min with an increased CaO content in the catalyst system. Similar total hydrogen production values (around 14.5 mmol H$_2$ g^{-1} biomass) were also obtained for the Ni–Mg–Al–0.5CaO and Ni–Mg–Al–2CaO catalysts (Table 2). In addition, the concentration of CH$_4$ from the online gas analysis also showed similar levels for the two catalysts; this is also consistent with the observations from the off-line gas chromatographic analysis (Table 2).

Catalytic reforming (Route 1 in Fig. 4) for total hydrogen production is suggested to be reduced due to the reduction of Ni–Mg–Al content by changing the catalyst from the Ni–Mg–Al–0.5CaO to Ni–Mg–Al–2CaO. However, here we obtained similar levels of production of H$_2$ for the Ni–Mg–Al–0.5CaO and Ni–Mg–Al–2CaO catalysts. This further suggests that the CaO was effective for the enhancement of hydrogen production during biomass gasification by *in situ* adsorption of CO$_2$. Furthermore, the reduction of CO and CO$_2$ content (Fig. 5) using the Ni–Mg–Al–2CaO catalyst indicates that the CaO in the catalyst system plays an important role in the *in situ* CO$_2$ adsorption and contributed to the Route 2 reaction (Fig. 4) for hydrogen production, where the water–gas shift reaction (eqn (2)) was promoted.

From the above discussion, it is suggested that the addition of CaO to the Ni–Mg–Al catalyst system could contribute to the enhancement of hydrogen production, while the catalytic Ni sites were reduced by the reduction of the Ni–Mg–Al content due to dilution by CaO. However, the optimum ratio of CaO was 20 wt% CaO in this work, which produced the maximum hydrogen production (proposed in Fig. 4); too high a CaO content will reduce the hydrogen production due to the relative reduction of the catalytic Ni sites.

3.3 TPO results of reacted Ni–Mg–Al–CaO catalyst/sorbent

The reacted Ni–Mg–Al–CaO catalyst/sorbent samples produced from the pyrolysis catalytic gasification of wood were characterised using TGA-TPO. A FTIR instrument was connected to the TPO analysis to identify CO$_2$ release. Fig. 6 shows TGA-TPO and TGA-CO$_2$ absorbance peak results of the reacted Ni–Mg–Al catalyst with different contents of CaO. The weight increase which occurred at around 450 °C in Fig. 6(a) could be assigned to the oxidation of Ni particles during the TPO experiment.

During TGA-TPO analysis, the weight loss occurred at around 100 °C, which was due to the moisture loss of the reacted catalyst. Carbon oxidation resulted in a weight loss that occurred at round 450 °C and was ascribed to the oxidation of amorphous carbons deposited on the reacted catalyst.[23] Carbon oxidation occurred at around 550 °C and was suggested to be the oxidation of filamentous carbons deposited on the reacted catalyst.[23,24] The weight loss at a temperature of around 750 °C was suggested to be decomposition of $CaCO_3$ (eqn (6)).

As shown in Fig. 6(a), the amount of carbon deposited on the catalyst/sorbent sample decreased as the CaO content was increased from 11.1 to 33.3 wt%. According to the results presented in Table 2, as the CaO content was increased, the concentrations of the hydrocarbons (C_1 to C_4) increased; indicating that carbon formation from hydrocarbon cracking was depressed. It is also suggested that increasing the CaO content used in the gasification stage might enhance the steam gasification of carbon deposited on the surface of the catalyst/sorbent sample (eqn (7)):

$$C + 2H_2O \rightarrow CO_2 + 2H_2 \tag{7}$$

However, there might be an overlap with the oxidation of carbons (weight loss) and oxidation of Ni (weight increase) during the TPO analysis. Fig. 6(b) shows the CO_2 release obtained from downstream FTIR analysis; thus oxidation of the carbons could be indicated from CO_2 release. Significant changes were detected as a result of increasing the CaO content. CO_2 release before the oxidation temperature of 650 °C (carbon oxidation) was much lower for the reacted catalyst with CaO addition, compared with the reacted Ni–Mg–Al catalyst. It is demonstrated that the addition of CaO to the Ni–Mg–Al catalyst was effective for the reduction of carbon deposition during biomass gasification.

Additionally, more CO_2 gas was released due to the decomposition of $CaCO_3$ (eqn (6)) which was obtained from Fig. 6(b), when more CaO was present in the Ni–Mg–Al–CaO catalyst system. Therefore, the addition of CaO showed an effect on *in situ* CO_2 adsorption during the gasification process.

The improvement of the reduction of coke deposition on the reacted catalyst due to CaO addition was also shown from the FTIR spectra connected with TPO (Fig. 7). Since it was clearly seen from the FTIR spectra that the CO_2 emission was reduced with an increased CaO content, and more CO_2 was released at the end of the TPO analysis ($CaCO_3$ decomposition).

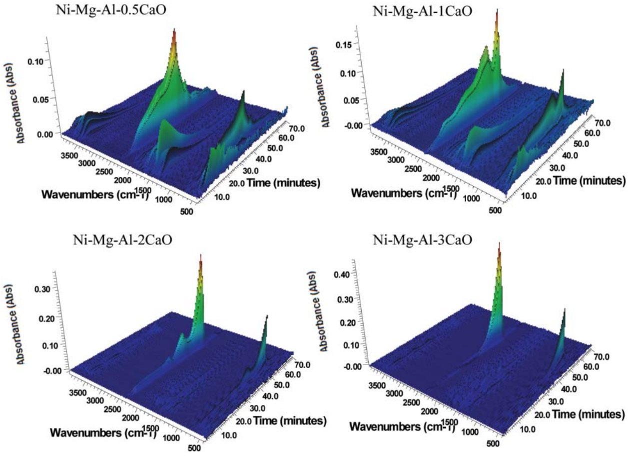

Fig. 7 TGA-FTIR thermograms representing absorbance with respect to time and wave number for the reacted Ni–Mg–Al–CaO catalyst/sorbent.

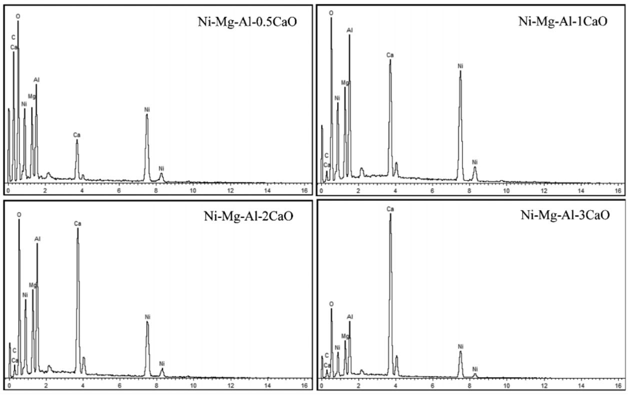

Fig. 8 EDXS results of the reacted Ni–Mg–Al catalyst with different contents of CaO.

Fig. 8 shows the EDXS spectrograms of the reacted Ni–Mg–Al and Ni–Mg–Al–CaO catalysts. The EDXS analysis (semi-quantity method) confirmed the presence of the basic elements (C, Ni, O, Ca, Mg and Al) in the reacted catalysts. It is shown that a much lower carbon deposition was observed on the reacted Ni–Mg–Al–CaO catalysts compared with the reacted Ni–Mg–Al catalyst; this is consistent with the results from TGA-TPO analysis (Fig. 6).

We have shown in this work that CaO for CO_2 adsorption, in combination with Ni catalysis, is effective for the production of high yield hydrogen gas. However, there is an optimum amount of CaO which can be added to the catalyst before the relative amount of Ni becomes reduced by dilution, resulting in a decrease in the effectiveness of the Ni catalyst and consequently reduced hydrogen production. The CaO can be easily added to the Ni catalyst as part of the preparation process. Balancing the CaO and Ni contents of the catalyst/sorbent can reduce the amount of Ni added, consequently reducing the Ni costs, but producing the same overall yield of hydrogen.

4. Conclusions

In this paper, a novel bi-functional Ni–Mg–Al–CaO catalyst/sorbent has been prepared with different contents of CaO. The prepared catalysts were tested for hydrogen production from the pyrolysis-gasification of wood biomass by using a two-stage fixed-bed reaction system. The results showed the following conclusions:

Carbonation/calcination results using TGA analysis in the presence of a N_2 or CO_2 atmosphere showed that the reactivity of CaO for CO_2 adsorption decreased after several carbonation/calcination cycles, while the Ni–Mg–Al–CaO catalyst showed a comparatively stable carbonation conversion after 20 carbonation/calcination cycles. Thus, the stability of CO_2 adsorption for CaO was enhanced when CaO was incorporated into the Ni–Mg–Al catalyst.

The increase of CaO content in the Ni–Mg–Al catalyst system was found to increase the H_2/CO ratio during biomass gasification. For example, the H_2/CO ratio was increased from 0.128 to 0.160 g g^{-1}, when the CaO content was increased from 0 to 42.9 wt% in the Ni–Mg–Al–CaO catalyst system.

Hydrogen production was suggested to be controlled by two main routes: (1) hydrocarbon conversion and (2) water–gas shift reaction enhanced by CO_2 adsorption. When the catalyst was changed from Ni–Mg–Al to Ni–Mg–Al–0.5CaO, hydrogen production was reduced from 20.4 to 15.3 (mmol g^{-1} biomass), which suggested that hydrocarbon conversion to H_2 was depressed by the relative reduction of the Ni content. However, with the increase of the CaO ratio (Ni–Mg–Al–1CaO), hydrogen production was increased to 20.2 (mmol g^{-1} biomass). This is ascribed to the dominant water–gas shift reaction, enhanced by the CO_2 adsorption of CaO. With further increases of the CaO content in the Ni–Mg–Al–CaO system, hydrogen production was reduced due to the catalytic conversion of hydrocarbons to H_2 being reduced by the reduction of the overall Ni content.

Reacted catalysts characterized by TPO-FTIR results showed that carbon deposition was significantly reduced when CaO was added to the Ni–Mg–Al catalyst. In addition, carbon deposition was also found to be reduced with an increased CaO content in the catalyst system.

Acknowledgements

This work was supported by the UK Engineering and Physical Sciences Research Council under EPSRC Grant EP/D053110/1, National Natural Science Foundation of China (no. 50930006), and the Key Technologies R&D Program of China (No. 2011BAD15B05-03). The authors also thank the Analytical and Testing Center of Huazhong University of Science and Technology for SEM analysis.

Notes and references

1 S. Koppatz, C. Pfeifer, R. Rauch, H. Hofbauer, T. Marquard-Moellenstedt and M. Specht, *Fuel Process. Technol.*, 2009, **90**, 914–921.
2 J. Werther, M. Saenger, E. U. Hartge, T. Ogada and Z. Siagi, *Prog. Energy Combust. Sci.*, 2000, **26**, 1–27.
3 A. Abuadala and I. Dincer, *Int. J. Energy Res.*, 2012, **36**, 415–455.
4 P. N. Sheth and B. V. Babu, *Int. J. Hydrogen Energy*, 2010, **35**, 10803–10810.
5 Q. Xie, S. Kong, Y. Liu and H. Zeng, *Bioresour. Technol.*, 2012, **110**, 603–609.
6 C. Wu, L. Wang, P. T. Williams, J. Shi and J. Huang, *Appl. Catal., B*, 2011, **108–109**, 6–13.
7 B.-S. Huang, H.-Y. Chen, K.-H. Chuang, R.-X. Yang and M.-Y. Wey, *Int. J. Hydrogen Energy*, 2012, **37**, 6511–6518.
8 P. Lv, Z. Yuan, C. Wu, L. Ma, Y. Chen and N. Tsubaki, *Energy Convers. Manage.*, 2007, **48**, 1132–1139.
9 R. Isha and P. T. Williams, *J. Energy Inst.*, 2011, **84**, 80–87.
10 S. Lin, M. Harada, Y. Suzuki and H. Hatano, *Energy Convers. Manage.*, 2005, **46**, 869–880.
11 C. Wu and P. T. Williams, *Fuel*, 2010, **89**, 1435–1441.
12 B. Dou, Y. Song, Y. Liu and C. Feng, *J. Hazard. Mater.*, 2010, **183**, 759–765.
13 M. R. Mahishi and D. Y. Goswami, *Int. J. Hydrogen Energy*, 2007, **32**, 2803–2808.
14 M. Broda, A. M. Kierzkowska, D. Baudouin, Q. Imtiaz, C. Copéret and C. R. Müller, *ACS Catal.*, 2012, **2**, 1635–1646.
15 J. Kobayashi, K. Kawamoto, R. Fukushima and S. Tanaka, *Chemosphere*, 2011, **83**, 1273–1278.
16 L. Garcia, A. Benedicto, E. Romeo, M. L. Salvador, J. Arauzo and R. Bilbao, *Energy Fuels*, 2002, **16**, 1222–1230.
17 Z.-s. Li, N.-s. Cai and Y.-y. Huang, *Ind. Eng. Chem. Res.*, 2006, **45**, 1911–1917.
18 V. Manovic and E. J. Anthony, *Environ. Sci. Technol.*, 2007, **41**, 1420–1425.
19 D. Alvarez and J. C. Abanades, *Ind. Eng. Chem. Res.*, 2005, **44**, 5608–5615.
20 H. Lu, E. P. Reddy and P. G. Smirniotis, *Ind. Eng. Chem. Res.*, 2006, **45**, 3944–3949.
21 M. Widyawati, T. L. Church, N. H. Florin and A. T. Harris, *Int. J. Hydrogen Energy*, 2011, **36**, 4800–4813.
22 L. Han, Q. Wang, Y. Yang, C. Yu, M. Fang and Z. Luo, *Int. J. Hydrogen Energy*, 2011, **36**, 4820–4829.
23 C. Wu and P. T. Williams, *Appl. Catal., B*, 2010, **96**, 198–207.
24 P. Wang, E. Tanabe, K. Ito, J. Jia, H. Morioka, T. Shishido and K. Takehira, *Appl. Catal., A*, 2002, **231**, 35–44.